Spin interference effects in ring conductors subject to Rashba coupling

Diego Frustaglia*
Institut für Theoretische Festkörperphysik, Universität Karlsruhe, 76128 Karlsruhe, Germany

Klaus Richter
Institut für Theoretische Physik, Universität Regensburg, 93040 Regensburg, Germany
(Received 9 September 2003; revised manuscript received 11 February 2004; published 10 June 2004)

Quantum interference effects in rings provide suitable means for controlling spin at mesoscopic scales. Here we apply such control mechanisms to coherent spin-dependent transport in one- and two-dimensional rings subject to Rashba spin-orbit coupling. We first study the spin-induced modulation of unpolarized currents as a function of the Rashba coupling strength. The results suggest the possibility of all-electrical spintronic devices. Moreover, we find signatures of Berry phases in the conductance previously unnoticed. Second, we show that the polarization direction of initially polarized, transmitted spins can be tuned via an additional small magnetic control flux. In particular, this enables to precisely reverse the polarization direction at half a flux quantum. We present full numerical calculations for realistic two-dimensional ballistic microstructures and explain our findings in a simple analytical model for one-dimensional rings.

DOI: 10.1103/PhysRevB.69.235310 PACS number(s): 73.23.−b, 03.65.Vf, 72.10.−d, 72.25.−b

I. INTRODUCTION

In the last decade the field of *quantum electronics*[1,2] has received extraordinary attention from both experimental and theoretical physics communities. Special effort has been made towards control and engineering of the spin degree of freedom at the mesoscopic scale, usually referred to as *spintronics*.[3,4] The major problem faced in this field is the generation of spin-polarized carriers and their appropriate manipulation in a controllable environment, preferably in semiconductors. Since the original proposal of the spin field effect transistor by Datta and Das,[5] significant progress has been made[6] though the realization of a spin transistor still remains as a challenge. Setups based on intrinsic spin-dependent properties of semiconductors, as the Rashba effect[7,8] for a two-dimensional electron gas confined to an asymmetric potential well, appear to be of particular interest owing to the convenient means of all-electrical control through additional gate voltages.[9] In addition, coherent ring conductors enable to exploit the distinct interference effects of electron spin *and* charge which arise in these doubly connected geometries. This opens up the area of spin-dependent Aharonov-Bohm physics, including topics such as Berry phases,[10,11] spin-related conductance modulation,[12,13] persistent currents,[14,15] spin filters[16] and detectors,[17] spin rotation,[18,19] and spin switching mechanisms.[20–22]

In this paper we focus on two different aspects of spin interference in ballistic one- and two-dimensional (1D and 2D) ring geometries subject to Rashba spin-orbit coupling.[29] First, motivated by the work of Nitta *et al.*,[12] in Sec. II we revisit the subject of spin-induced modulation of unpolarized currents using the Hamiltonian for 1D rings recently introduced by Meijer *et al.*,[32] which sligtly differs from the one used previously.[12,24,33] Taking into account the corresponding appropriate eigenstates, we derive in Sec. III the modulation profile of the conductance as a function of the Rashba coupling strength and extract distinct effects due to the presence of Berry phases which have not been recognized in earlier work.[12] The 1D results are later compared with independent fully numerical calculations for 2D rings. The imprints of the Rashba coupling (strength) on the overall conductance is remarkable, pointing towards the possibility of all-electrical spintronics devices.

Second, and motivated by our previous work on spin control in the presence of external inhomogeneous magnetic fields,[20] we study in Sec. IV the magnetoconductance of initially spin-polarized carriers traversing a ring geometry with Rashba spin-orbit interaction. We demonstrate by means of numerical calculations for 2D ring systems that the spin orientation of polarized carriers can be tuned and even reversed by means of an additional small magnetic control field. This implies a spin-switching mechanism which is probably more convenient for experimental realizations than our previous proposal,[20] since the originally suggested external inhomogeneous magnetic field is now replaced by the intrinsic effective field due to the Rashba interaction.

After a short summary in Sec. V we present details of our analytical approach in an Appendix.

II. MODEL AND RELEVANT PARAMETERS

A. Hamiltonian

The 2D quantum Hamiltonian for particles of charge $-e$ ($e>0$) and effective mass m^* subject to Zeeman and Rashba coupling with coupling constants μ and α_R, respectively, reads

$$H_{2D} = \frac{1}{2m^*}\mathbf{\Pi}^2 + \mu\mathbf{B}\cdot\boldsymbol{\sigma} + \frac{\alpha_R}{\hbar}(\boldsymbol{\sigma}\times\mathbf{\Pi})_z + V(\mathbf{r}), \qquad (1)$$

where $\boldsymbol{\sigma}$ is the vector of the Pauli spin matrices, $\mathbf{\Pi}=\mathbf{p}+(e/c)\mathbf{A}$, and $\mathbf{B}=\boldsymbol{\nabla}\times\mathbf{A}$. The electrostatic potential $V(\mathbf{r})$ defines, e.g., the confining potential of a 2D ballistic conductor. Recently it has been shown[32] that taking the limit from 2D to 1D rings [Fig. 1] has to be performed by carefully consider-

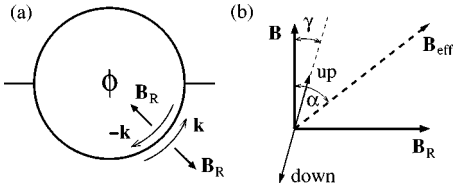

FIG. 1. (a) 1D ring of radius r_0 subject to Rashba coupling in the presence of an additional, vertical magnetic field $\mathbf{B}$ (flux $\phi = \pi r_0^2 B$). Spin carriers traveling around the ring see a momentum ($\mathbf{k}$) dependent in-plane Rashba field $\mathbf{B}_R$, which is orientationally inhomogeneous. (b) Up and down spin eigenstates do not generally align with the total effective field $\mathbf{B}_{\text{eff}} = \mathbf{B} + \mathbf{B}_R$.

ing in the above Hamiltonian (1) the radial wave functions in the presence of a narrow confinement. As a consequence, the corresponding 1D Hamiltonian for a ring of radius r_0 in the presence of a vertical magnetic field $\mathbf{B}=(0,0,B)$ reads[32,34]

$$H_{1D} = \frac{\hbar\omega_0}{2}\left(-i\frac{\partial}{\partial\varphi} + \frac{\phi}{\phi_0}\right)^2 + \frac{\hbar\omega_B}{2}\sigma_z + \frac{\hbar\omega_R}{2}(\cos\varphi\,\sigma_x + \sin\varphi\,\sigma_y)\left(-i\frac{\partial}{\partial\varphi} + \frac{\phi}{\phi_0}\right) - i\frac{\hbar\omega_R}{4}(\cos\varphi\,\sigma_y - \sin\varphi\,\sigma_x), \tag{2}$$

where we have introduced the polar angle φ, the frequencies $\omega_0 = \hbar/(m^* r_0^2)$, $\omega_B = 2\mu B/\hbar$, and $\omega_R = 2\alpha_R/(\hbar r_0)$, and the magnetic fluxes $\phi = \pi r_0^2 B$ and $\phi_0 = hc/e$.

The 1D eigenstates of Eq. (2) have the general form

$$\Psi^s_{\lambda,n}(\varphi) = \exp(i\lambda n\varphi)\chi^s_{\lambda,n}; \quad \chi^s_{\lambda,n} = \begin{pmatrix} \chi_1 \\ \chi_2 \quad e^{i\varphi} \end{pmatrix}. \tag{3}$$

Here, the spin components $\chi_{1,2}$ depend, in principle, on the travel direction $\lambda = \pm 1$, orbital quantum number $n \geqslant 0$ (n integer), and spin $s = \pm 1$. The spin carriers being subject to H_{1D} experience an effective magnetic field $\mathbf{B}_{\text{eff}} = \mathbf{B} + \mathbf{B}_R$ composed of the external field $\mathbf{B}$ and the momentum dependent field $\mathbf{B}_R$ arising from the Rashba coupling. $\mathbf{B}_R$ lies in the plane of the ring. $\mathbf{B}_{\text{eff}}$ encloses a tilt angle α with the z axis given by $\tan\alpha = B_R/B = \omega_R(n'+1/2)/\omega_B$ with $n' = \lambda n + \phi/\phi_0$ (see the Appendix for further details). The exact orientation of $\mathbf{B}_R$ is determined by the magnitude and sign of the momentum, namely λn, i.e., spins traveling in opposite directions are subject to a different $\mathbf{B}_R$. Moreover, Eq. (2) implies that the orientation of $\mathbf{B}_{\text{eff}}$ varies spatially.[35] This means that, in general, the corresponding spin eigenstates (3) are *not aligned* with $\mathbf{B}_{\text{eff}}$ [see Fig. 1(b)]. On the contrary, they are characterized by a different tilt angle γ determined by the relative magnitude of the spinor components χ_1 and χ_2. However, in the limit of strong spin-orbit coupling, the so-called *adiabatic* regime, the spin eigenstates follow the local direction of the effective field, and $\gamma \to \alpha$ (leading to Berry phases[10]). This limit is reached if the adiabaticity parameter $Q = Q_B + Q_R$ satisfies $Q \gg 1$,[23,24] where we have defined $Q_B = \omega_B/(\omega_0|n'+1/2|)$ and Q_R, particularly relevant here, as

$$Q_R = \omega_R/\omega_0. \tag{4}$$

Hence, the adiabatic limit corresponds to the situation where a spin precesses many times during a full travel around the ring.

B. 1D eigenstates in the absence of an external magnetic field

For $\mathbf{B}=0$ we have $\omega_B = 0$ and $\phi = 0$ in Eq. (2), and the Hamiltonian H_{1D} simplifies considerably. The resulting effective field reduces to the in-plane field $\mathbf{B}_{\text{eff}} = \mathbf{B}_R$ with tilt angle $\alpha = \pi/2$. In this situation, the 1D eigenstates (3) take the simple form (see the Appendix for details)

$$\Psi^{\uparrow}_{+,n}(\varphi) = \exp(in\varphi)\begin{pmatrix} \sin\gamma/2 \\ \cos\gamma/2 \quad e^{i\varphi} \end{pmatrix}, \tag{5}$$

$$\Psi^{\downarrow}_{+,n}(\varphi) = \exp(in\varphi)\begin{pmatrix} \cos\gamma/2 \\ -\sin\gamma/2\; e^{i\varphi} \end{pmatrix}, \tag{6}$$

$$\Psi^{\uparrow}_{-,n}(\varphi) = \exp(-in\varphi)\begin{pmatrix} \cos\gamma/2 \\ -\sin\gamma/2 \quad e^{i\varphi} \end{pmatrix}, \tag{7}$$

$$\Psi^{\downarrow}_{-,n}(\varphi) = \exp(-in\varphi)\begin{pmatrix} \sin\gamma/2 \\ \cos\gamma/2 \quad e^{i\varphi} \end{pmatrix}. \tag{8}$$

The corresponding tilt angle γ is given by $\tan\gamma = Q_R$, satisfying $\gamma \to \alpha = \pi/2$ in the adiabatic limit $Q_R \to \infty$. Hence, we note that the spinors $\chi^s_{\lambda,n}$ in Eqs. (5)–(8) do not actually depend on n. Moreover, the associated eigenenergies read

$$E^s_{\lambda,n} = \frac{\hbar\omega_0}{2}\left[\left(\lambda n + \frac{1}{2}\right)^2 + \frac{1}{4} + s\left|\lambda n + \frac{1}{2}\right|\sqrt{1+Q_R^2}\right]. \tag{9}$$

The above spin eigenstates Eqs. (5)–(8), are defined in such a way that the eigenenergies (9) are maximum for spin-up states. We will make use of these results in the following section for the study of transport properties.

III. RASHBA MODULATION OF UNPOLARIZED CURRENTS

We first consider the case where the 1D ring of Sec. II B is symmetrically coupled to two contact leads [Fig. 1(a)] in order to study the transport properties of the system subject to a constant, low bias voltage (linear regime). To this end we calculate the zero-temperature conductance G based on the Landauer formula[36]

$$G = \frac{e^2}{h}\sum_{m',m=1}^{M}\sum_{\sigma',\sigma} T^{\sigma'\sigma}_{m'm}, \tag{10}$$

where $T^{\sigma'\sigma}_{m'm}$ denotes the quantum probability of transmission between incoming (m,σ) and outgoing (m',σ') asymptotic states defined on semi-infinite ballistic leads. The labels m,m' and σ,σ' refer to the corresponding mode and spin quantum numbers, respectively. For 1D rings [$M=1$ in Eq. (10)] the transmission coefficients can be approximated to first order as follows: In the presence of Rashba coupling the

energy splitting is such that particles with Fermi energy E_F can traverse the ring with four different wave numbers n_λ^s, depending on spin (s) and direction of motion (λ). The quantities n_λ^s are obtained by solving $E_{\lambda,n}^s = E_F$ in Eq. (9) and do not require to be integer. Moreover, in this simple approach we assume perfect coupling between leads and ring (i.e., fully transparent contacts), neglecting backscattering effects leading to resonances. Thus, incoming spins $|\sigma\rangle$ entering the ring at $\varphi = 0$ propagate coherently along the four available channels and interfere at $\varphi = \pi$, leaving the ring in a mixed spin state $|\sigma_{\text{out}}\rangle = \Sigma_{\lambda,s} \langle \chi_\lambda^s(0)|\sigma\rangle \exp(i n_\lambda^s \pi)|\chi_\lambda^s(\pi)\rangle$.[37] Choosing a complete basis of incoming and outgoing spin states, the spin-resolved transmission probabilities are obtained as $T^{\sigma'\sigma} = |\langle \sigma' | \sigma_{\text{out}}\rangle|^2$. After summation over the spin indices σ and σ', we obtain for the total conductance

$$G = \frac{e^2}{h}\left[1 + \frac{1}{2}[\cos\ \pi(n_-^\downarrow - n_+^\uparrow) + \cos\ \pi(n_-^\uparrow - n_+^\downarrow)]\right]. \quad (11)$$

Note that the phase difference acquired by opposite spin states traveling in opposite directions plays an important role for the modulation of the conductance.[38] The spin-dependent phases are signatures of the Aharonov-Casher effect[39] for spins traveling in the presence of an electric field, which is the electromagnetic dual of the Aharonov-Bohm effect.

By imposing $E_{\lambda,n}^s = E_F$ in Eq. (9) we obtain

$$(n_-^\downarrow - n_+^\uparrow) = 1 + \sqrt{1 + Q_R^2}, \quad (12)$$

$$(n_-^\uparrow - n_+^\downarrow) = 1 - \sqrt{1 + Q_R^2}. \quad (13)$$

Inserting the above expressions into Eq. (11) one finds the total conductance as a function of the dimensionless Rashba coupling strength Q_R,

$$G = \frac{e^2}{h}\{1 + \cos[\pi(\sqrt{1 + Q_R^2} - 1)]\} \quad (14)$$

$$= \frac{e^2}{h}\{1 + \cos[\pi Q_R \sin\ \gamma - \pi(1 - \cos\ \gamma)]\}, \quad (15)$$

where we used $\tan\ \gamma = Q_R$, $\cos\ \gamma = 1/\sqrt{1+Q_R^2}$, and $\sin\ \gamma = Q_R/\sqrt{1+Q_R^2}$. Comparing Eq. (14) with the corresponding result of Nitta, Meijer, and Takayanagi,[12]

$$G_{\text{NMT}} = \frac{e^2}{h}[1 + \cos(\pi Q_R)], \quad (16)$$

we recognize two main contributions to the phase in Eq. (15): One is the Rashba phase $\varphi_R = \pi Q_R \sin\ \gamma$. This is similar to the phase πQ_R (Ref. 40) appearing in G_{NMT}, Eq. (16), but corrected by a factor $\sin\ \gamma$ accounting for the fact that the spinors are generally not aligned with $\mathbf{B}_{\text{eff}}$. In the limit of adiabatic spin transport both phases coincide (since $\sin\ \gamma \to 1$ as $Q_R \to \infty$). Moreover, we find an additional Aharonov-Anandan phase[42] contribution $\varphi_{AA} = \pi(1 - \cos\ \gamma)$ to Eq. (15) absent in G_{NMT} and related to the solid angle accumulated by the change of spinor orientation during transport. In the adiabatic limit, φ_{AA} tends to the corresponding Berry phase $\varphi_B = \pi(1 - \cos\ \alpha)$ as $\cos\ \gamma \to \cos\ \alpha$ (where $\cos\ \alpha = 0$, i.e., $\varphi_B = \pi$ in the present case).

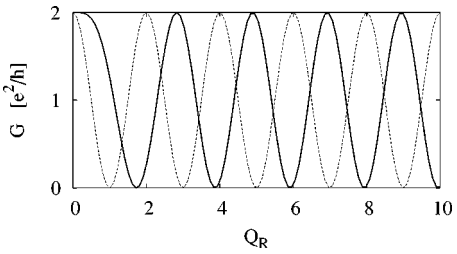

FIG. 2. Conductance-modulation profile of 1D rings [Fig. 1(a)] as a function of the dimensionless Rashba strength Q_R in the absence of external magnetic field ($\mathbf{B} = 0$). The curves show our result (14) for G (solid line) compared to the originally incomplete G_{NMT} of Eq. (16) (dashed line).

In Fig. 2 we plot for comparison our result, Eq. (14), for G together with G_{NMT}, Eq. (16), as a function of the Rashba strength Q_R. There we observe that while G_{NMT} (dashed line) shows regular oscillations of period 2 in Q_R units, our result (solid line) exhibits quasiperiodic oscillations of period larger than 2 reflecting the fact that nonadiabatic spin transport ($\sin\ \gamma < 1$) takes place for small Q_R. For $Q_R \gg 1$ the period is tending to 2 as the adiabatic limit is approached. In addition, a relative phase shift of magnitude π survives between G and G_{NMT} for large Q_R, coinciding with the appearance of the Berry phase $\varphi_B = \pi$. As a consequence, minima in G are obtained for even integers of $\sqrt{Q_R^2 + 1}$, i.e., $Q_R = \sqrt{3}, \sqrt{15}, \ldots$. These minima are reminiscent of those found for the conductance of rings subject to Zeeman spin-coupling to in-plane circular magnetic fields (instead of Rashba coupling) as a function of the corresponding adiabaticity parameter.[20] Moreover, we note that Eq. (16), predicting uniform oscillations as a function of the coupling strength, actually corresponds to the conductance of a 1D ring subject to a radial electric field of constant magnitude (instead of a vertical one as in the case of Rashba coupling).[33,43]

To complete the above discussion we present in the following the results of independent numerical calculations corresponding to more realistic 2D ring structures (Fig. 3). To this end we calculate the zero-temperature conductance G based on the Landauer formula (10) by using a spin-dependent recursive Green-function technique[44] applied to the 2D Hamiltonian (1). Unless otherwise stated, our numerical calculations correspond to a quantum transmission aver-

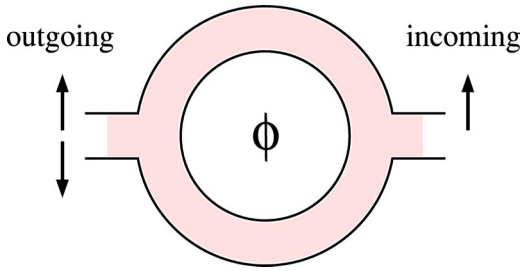

FIG. 3. 2D ring of mean radius r_0 and width w used for numerical calculations of the conductance. The gray zone corresponds to the region subject to a finite Rashba coupling. This is switched on and off adiabatically within the leads by using a linear function. An additional, vertical magnetic field $\mathbf{B}$ generates a flux $\phi = \pi r_0^2 B$.

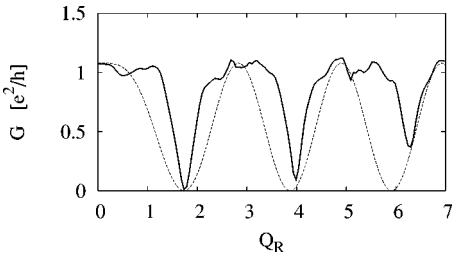

FIG. 4. Numerical calculation of the conductance-modulation profile (solid line) of a single-mode 2D ring (Fig. 3, aspect ratio $w/r_0 \approx 0.3$) as a function of the dimensionless Rashba strength Q_R in the absence of an external magnetic field ($\mathbf{B}=0$). Dashed line: corresponding 1D result, Eq. (14) (same as the solid line in Fig. 2) including a fitting prefactor at $Q_R=0$ for comparison.

aged within a small energy window[47] in order to smooth out energy-dependent oscillations related to resonances in the ring structure. Moreover, the Rashba coupling is switched on and off adiabatically[48] within the leads by using a linear function.[49] Figure 4 (solid line) shows the result for a single-mode ring of mean radius r_0 and width w (aspect ratio $w/r_0 \approx 0.3$) symmetrically coupled to two leads of the same width (see Fig. 3). This result is to be compared with that for the strictly 1D ring of Eq. (14) (dashed line; overall scaling factor included). Both curves present similar features on the whole. We observe that the first minimum of G in Fig. 4 coincides for both 1D and 2D calculations. However, as Q_R increases the 2D minima (solid line) undergo a small relative shift with respect to the 1D result (dashed line) and get less pronounced. This can be related to the finite aspect ratio of the ring: The strength Q_R can actually be written as $Q_R = (r_0/w)\delta_R$, where $\delta_R = \alpha_R(2m^*/\hbar^2)w$ is the parameter defining the strength of the Rashba coupling in 2D conducting wires of width w.[5,41] The weak-coupling regime characterized by spin subband separation is defined for $\delta_R \ll 1$. For the case of 1D wires and rings, this condition is always satisfied since $w=0$. For finite width (represented by the finite w/r_0 in our case) the situation is different, as we verify in our results of Fig. 4. There, the first minimum at $Q_R=\sqrt{3}$ (fitting the above 1D result) corresponds to a relatively small coupling strength $\delta_R \approx 0.5$. However, at the second minimum, $Q_R \approx 4 > \sqrt{15}$, we already enter the strong-coupling regime with $\delta_R \approx 1.2$. As a consequence deviations from the 1D case in the corresponding conductance-modulation profile arise. This tendency is less pronounced as $w/r_0 \to 0$ and the parameter δ_R losses relevance.

Moreover, we note that in Fig. 4 the conductance minima of finite width rings (solid line) suffer the shift to *larger* values of Q_R with respect to the 1D results (dashed line) as Q_R increases. This suggests that the radial motion in 2D rings obstructs the approach to the regime of adiabatic spin transport, since a relatively larger coupling Q_R would be necessary for obtaining the same spinor tilt angle γ according to the structure of the phase (15).

Additionally, numerical results[50] not presented here indicate that the conductance of 2D ring structures supporting several open channels shows a modulation pattern similar to that of Fig. 4 provided that (i) the incoming and outgoing leads support just one open channel and (ii) the corresponding aspect ratio is small ($w/r_0 \ll 1$). Furthermore, ring structures of irregular shape (leading to ballistic backscattering enhancement) exhibit a halfing of the period in $G(Q_R)$ modulation profiles when compared with that of Fig. 4, similar to what is predicted for disordered systems.[43,51,52]

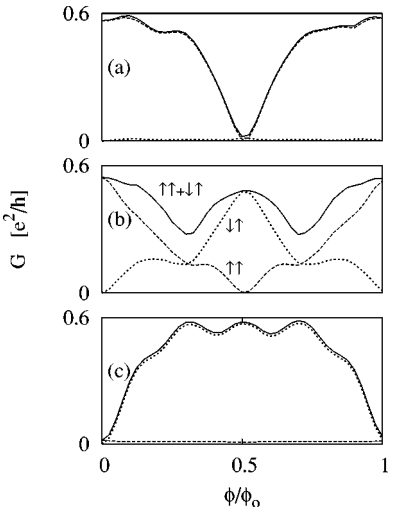

FIG. 5. Numerical results for the conductance of spin-up polarized incoming carriers (see Fig. 3) through a single-mode 2D ring (aspect ratio $w/r_0 \approx 0.3$) as a function of a flux $\phi = \pi r_0^2 B$ in the presence of Rashba coupling of increasing strength: $Q_R \approx 0.2$ (a), 1.0 (b), and 1.7 (c) (see Fig. 4 for comparison at $\phi=0$). The overall conductance (solid line) is split into its components $G^{\uparrow\uparrow}$ (dashed) and $G^{\downarrow\uparrow}$ (dotted). Note the continuous change of the spin polarization with ϕ and the spin switching at $\phi=\phi_0/2$.

IV. MAGNETOCONDUCTANCE OF SPIN-POLARIZED CURRENTS AND SPIN SWITCHING

In this section we discuss the possibility of controlling the spin orientation of *spin-polarized* carriers by means of distinct interference effects in mesoscopic ring structures due to (charge and spin) quantum coherence. Motivated by our previous work on spin switching in the presence of in-plane circular magnetic fields[20] we study here the magnetoconductance of incoming spin-polarized carriers,[53] now subject to Rashba interaction.

The setup proposed is that of Fig. 3, representing a 2D ring (aspect ratio $w/r_0 \approx 0.3$) subject to Rashba coupling symmetrically coupled to two leads. In addition, a weak magnetic field **B** is applied along the vertical axis leading to a flux ϕ. Incoming and outgoing spin states are defined along the vertical axis as shown in Fig. 3. We consider spin-up polarized incoming particles[54] (equivalent results are obtained for spin-down incoming states). Using the recursive Green-function technique introduced in Sec. III we calculate numerically the spin-resolved conductances $G^{\uparrow\uparrow}$ and $G^{\downarrow\uparrow}$, corresponding to outgoing spin-up and -down channels, respectively (see Fig. 3). In order to smooth out energy-dependent oscillations, the present numerical calculations correspond to an energy-averaged quantum transmission in a small energy window.[47] Our main results for a single-mode ring are summarized in Fig. 5, showing the overall conduc-

tance (solid line) split into its components $G^{\uparrow\uparrow}$ (dashed line) and $G^{\downarrow\uparrow}$ (dotted line) as a function of the magnetic flux ϕ for three different scaled Rashba strengths $Q_R \approx 0.2$, 1.0, and 1.7. In the weak-coupling limit, Fig. 5(a), the overall conductance (solid line) shows the usual AB oscillations of period ϕ_0 and is dominated by $G^{\uparrow\uparrow}$ (dashed line). As expected for weak spin coupling, the spin polarization is almost conserved during transport.

More interesting features appear for the case of moderate coupling depicted in panel (b). There, both components $G^{\uparrow\uparrow}$ (dashed line) and $G^{\downarrow\uparrow}$ (dotted line) contribute similarly to the overall conductance (solid line). However, the spin polarization of the transmitted carriers changes continuously as a function of the magnetic flux ϕ: We note that $G^{\downarrow\uparrow}=0$ at $\phi=0$, while $G^{\uparrow\uparrow}=0$ at $\phi=\phi_0/2$. Hence, for zero flux all transmitted carriers conserve their original (incoming) spin orientation, while for $\phi=\phi_0/2$ the transmitted particles reverse their spin polarization. That means that by tuning the magnetic flux from 0 to $\phi_0/2$ we can reverse the spin polarization of transmitted particles in a controlled way. The setup of Fig. 3 (i.e., AB ring subject to Rashba coupling) acts as a tunable spin switch, similar to our previous proposal for AB rings subject to inhomogeneous magnetic fields[20] with the advantage that in the present system the spin-dependent (Rashba) coupling can be electrically controlled.[9] Moreover, such spin-switching mechanism is independent of the strength Q_R, which determines only the amplitude of the spin-reversed current (see below).

In addition to the above results we present in Fig. 5(c) calculations for a little larger strength $Q_R \approx 1.7$, corresponding to the vicinity of the first minimum in Fig. 4 for zero flux. There we see that the AB oscillations in the overall conductance (solid line) suffer a shift of $\phi_0/2$ with respect to the weak-coupling case of panel (a). This is due to the additional phase of order π acquired by the carriers for $Q_R \approx \sqrt{3}$ [see Eq. (14) and related paragraphs]. Moreover, the overall conductance is dominated by the spin-reversed component $G^{\downarrow\uparrow}$ (dotted line), while the complementary $G^{\uparrow\uparrow}$ (dashed line) is suppressed due to quantum interference.

As the coupling strength Q_R increases, we obtain a sequence of magnetoconductance profiles which reproduce periodically the different panels of Fig. 5, following the order (a)→(b)→(c)→(b)→(a)→(b)→(c)…. Such periodical feature is related to the unbounded accumulation of the Rashba phase in Eq. (15) as a function of Q_R. As a consequence, Fig. 5(a) is related to values of Q_R corresponding to maxima of the conductance in Fig. 4, while Fig. 5(c) is associated with the vicinity of the minima in Fig. 4. Figure 5(b), where the spin-switching effect appears most clearly, corresponds to intermediate values of Q_R lying between maxima and minima of the conductance in Fig. 4.

We point out that this mechanism for reversing the spin polarization does not rely on the spin coupling to the magnetic field **B** generating the control flux, as exploited via Zeeman splitting in spin filters. It is a pure quantum interference effect due to the cooperation between change and spin coherence during transport, which also exists for the nonaveraged conductance at a given energy. We further find that this effect also pertains for large values of the Rashba strength δ_R associated to wires of finite width w, indicating that radial motion does not affect the control mechanism for spin switching.

Additionally, further numerical calculations[50] for 2D ring structures supporting several open modes show features similar to that of Fig. 5 for single-mode rings, as long as (i) the incoming and outgoing leads support just one open channel and (ii) the corresponding aspect ratio is small ($w/r_0 \ll 1$). Deviations from, e.g., Fig. 5(b) arise as w/r_0 increases, manifested by a less defined minimum in $G^{\uparrow\uparrow}$ at $\phi=\phi_0/2$ due to the relatively large fraction of flux ϕ penetrating the finite-width ring in that case. Moreover, asymmetric rings with arms of different effective length can also show a flux-modulated spin polarization similar to that of Fig. 5(b). However, the spin switching is not complete, and it does not necessarily take place at $\phi=\phi_0/2$.

Analytical results for the spin switching in 1D rings can be, in principle, obtained by studying the spin-resolved transmission probabilities $T^{\sigma'\sigma}$ as defined in Sec. III.

V. CONCLUSIONS

We have studied coherent spin-dependent transport in ballistic 1D and 2D ring geometries subject to (spin-orbit) Rashba coupling. We first obtained, via analytical (1D) and numerical (2D) calculations, the spin-related conductance-modulation profile of *unpolarized* spin carriers as a function of the scaled Rashba strength Q_R, which also acts as a measure defining adiabatic spin transport for $Q_R \gg 1$. The conductance appears to be quite sensitive to Q_R, suggesting the possibility of all-electrical spintronic devices. Moreover, we point out the role played by Aharonov-Anandan and Berry phases unnoticed in a previous proposal.[12] In addition, we also studied the magnetoconductance of spin-polarized carriers to assess possibilities for controlling the spin orientation in the presence of Rashba coupling. We demonstrate that an additional small flux ϕ can be used as a control parameter for inducing spin flips. The mechanism arises from cooperative quantum interference of charge and spin degrees of freedom in coherent transport. Combined with a spin detector such a device may be used for controlling spin-polarized currents alternative to the Datta-Das transistor.[5] Moreover, we note that the Dresselhaus spin-orbit coupling,[30] not studied here, could lead to similar conductance-modulation and spin-switching effects. However, its interplay with the Rashba coupling in systems where both contributions are comparable can produce further effects of interest.[31,55]

ACKNOWLEDGMENTS

We thank M. Governale, F. Meijer, J. Splettstoesser, and U. Zülicke for useful discussions. We acknowledge financial support from the Deutsche Forschungsgemeinschaft and thank the Max-Planck-Institut for the Physics of Complex Systems in Dresden, Germany, for providing computational resources.

APPENDIX: ID SPIN EIGENSTATES AND EFFECTIVE RASHBA FIELD

The components of the eigenstates $\Psi^s_{\lambda,n}$ of the 1D Hamiltonian (2), which are given in Eq. (3) (spin $s=\pm 1$, travel

direction $\lambda = \pm 1$, integer orbital number $n \geqslant 0$), satisfy the matrix equation

$$\begin{pmatrix} \frac{\hbar\omega_0}{2} n'^2 + \frac{\hbar\omega_B}{2} & \frac{\hbar\omega_R}{2}\left(n' + \frac{1}{2}\right) \\ \frac{\hbar\omega_R}{2}\left(n' + \frac{1}{2}\right) & \frac{\hbar\omega_0}{2}(n'+1)^2 - \frac{\hbar\omega_B}{2} \end{pmatrix} \chi = E^s_{\lambda,n}\chi, \tag{A1}$$

where the normalized spinors read

$$\chi = \begin{pmatrix} \chi_1 \\ \chi_2 \end{pmatrix} = \frac{1}{\sqrt{1 + (\Delta^s_{\lambda,n})^2}} \begin{pmatrix} 1 \\ \Delta^s_{\lambda,n} \end{pmatrix}, \tag{A2}$$

with

$$\Delta^s_{\lambda,n} = \frac{E^s_{\lambda,n} - (\hbar\omega_0/2)n'^2}{(\hbar\omega_R/2)(n' + 1/2)}, \tag{A3}$$

$n' = \lambda n + \phi/\phi_0$, and eigenvalues given by

$$E^s_{\lambda,n} = \frac{\hbar\omega_0}{2}\left\{\left[\left(n' + \frac{1}{2}\right)^2 + \frac{1}{4}\right] + s\sqrt{\left[\left(n' + \frac{1}{2}\right) - \frac{\omega_B}{\omega_0}\right]^2 + \left(\frac{\omega_R}{\omega_0}\right)^2\left(n' + \frac{1}{2}\right)^2}\right\}. \tag{A4}$$

The off-diagonal elements in the left-hand side of Eq. (A1) determine the magnitude and orientation of the in-plane effective Rashba field $\mathbf{B}_R$. The resulting overall effective field $\mathbf{B}_{\text{eff}} = \mathbf{B} + \mathbf{B}_R$ has a tilt angle α with respect to the z axis satisfying $\tan\alpha = \omega_R(n' + 1/2)/\omega_B$. Moreover, the presence of the kinetic terms in the diagonal elements of Eq. (A1) prevent the spinors χ to align with $\mathbf{B}_{\text{eff}}$. Instead, they are characterized by a tilt angle γ which tends to α only for strong spin coupling (adiabatic limit).

For illustration we discuss the spin-up case ($s = 1$) and the dependence on the travel direction λ in the absence of Zeeman coupling ($\omega_B = 0$, $\alpha = \pi/2$) provided that a finite flux ϕ is present. Then we find from Eq. (A2)

$$\chi^{\uparrow}_1 = \frac{Q_R}{\sqrt{2}[Q_{n'} + Q_R^2]^{1/2}}, \tag{A5}$$

$$\chi^{\uparrow}_2 = \frac{Q_{n'}}{\sqrt{2}[Q_{n'} + Q_R^2]^{1/2}}, \tag{A6}$$

where $Q_{n'} = 1 + \text{sgn}\,[n' + 1/2]\sqrt{1 + Q_R^2}$. The dimensionless Rashba strength Q_R is defined in Eq. (4). In the adiabatic, strong-coupling limit ($Q_R \gg 1$) we obtain from Eqs. (A5) and (A6)

$$\chi^{\uparrow} \overset{Q_R \gg 1}{\rightarrow} \begin{cases} \begin{pmatrix} 1/\sqrt{2}^- \\ 1/\sqrt{2}^+ \end{pmatrix} & \text{if} \quad \text{sgn}\,[n' + 1/2] = 1 \\ \begin{pmatrix} 1/\sqrt{2}^+ \\ -1/\sqrt{2}^+ \end{pmatrix} & \text{if} \quad \text{sgn}\,[n' + 1/2] = -1 \end{cases} \tag{A7}$$

indicating that the spinors are contained within the plane defined by the ring and pointing along $\mathbf{B}_R$. On the other hand, in the opposite limit of weak coupling ($Q_R \ll 1$), we arrive at

$$\chi^{\uparrow} \overset{Q_R \ll 1}{\rightarrow} \begin{cases} \begin{pmatrix} 0^+ \\ 1^- \end{pmatrix} & \text{if} \quad \text{sgn}\,[n' + 1/2] = 1 \\ \begin{pmatrix} 1^- \\ 0^- \end{pmatrix} & \text{if} \quad \text{sgn}\,[n' + 1/2] = -1 \end{cases} \tag{A8}$$

highlighting the influence of the traveling direction on the relative orientation of the spinors. As a consequence we find that the up spinors can be written as

$$\chi^{\uparrow} = \begin{cases} \begin{pmatrix} \sin\,\gamma/2 \\ \cos\,\gamma/2 \end{pmatrix} & \text{if} \quad \text{sgn}[n' + 1/2] = 1 \\ \begin{pmatrix} \cos\,\gamma/2 \\ -\sin\,\gamma/2 \end{pmatrix} & \text{if} \quad \text{sgn}[n' + 1/2] = -1 \end{cases} \tag{A9}$$

with $\tan\gamma = Q_R$. Following a similar procedure for $\phi = 0$ ($n' = \lambda n$) we find the eigenstates listed in Sec. II B.

*Present address: NEST-INFM & Scuola Normale Superiore, 56126 Pisa, Italy.

[1] L. L. Sohn, Nature (London) **394**, 131 (1998).
[2] *Mesoscopic Physics and Electronics*, edited by T. Ando, Y. Arakawa, K. Furuya, S. Komiyama, and H. Nakashima (Springer, Berlin, 1998).
[3] G. A. Prinz, Science **282**, 1660 (1998).
[4] S. A. Wolf, D. D. Awschalom, R. A. Buhrman, J. M. Daughton, S. von Molnár, M. L. Roukes, A. Y. Chtchelkanova, and D. M. Treger, Science **294**, 1488 (2001).
[5] S. Datta and B. Das, Appl. Phys. Lett. **56**, 665 (1990).
[6] For a recent account of the progress in the field see *Proceedings of the Second International Conference on Physics and Applications of Spin Related Phenomena in Semiconductors*, edited by L. W. Molenkamp, G. Schmidt, E. G. Novik, and H. Buhmann (Würzburg, 2002).
[7] E. I. Rashba, Fiz. Tverd. Tela (Leningrad) **2**, 1224 (1960) [Sov. Phys. Solid State **2**, 1109 (1960)].
[8] Y. A. Bychkov and E. I. Rashba, J. Phys. C **17**, 6039 (1984).
[9] J. Nitta, T. Akazaki, H. Takayanagi, and T. Enoki, Phys. Rev. Lett. **78**, 1335 (1997).
[10] M. V. Berry, Proc. R. Soc. London **392**, 45 (1984).
[11] Several theoretical proposals (Refs. 14, 20, and 22–26) as well as experimental realizations (Refs. 27 and 28) exist.
[12] J. Nitta, F. E. Meijer, and H. Takayanagi, Appl. Phys. Lett. **75**, 695 (1999).
[13] A. G. Mal'shukov, V. V. Shlyapin, and K. A. Chao, Phys. Rev. B **60**, R2161 (1999).
[14] D. Loss, P. Goldbart, and A. V. Balatsky, Phys. Rev. Lett. **65**, 1655 (1990).

[15] J. Splettstoesser, M. Governale, and U. Zülicke, Phys. Rev. B **68**, 165341 (2003).
[16] M. Popp, D. Frustaglia, and K. Richter, Nanotechnology **14**, 347 (2003).
[17] R. Ionicioiu and I. D'Amico, Phys. Rev. B **67**, 041307(R) (2003).
[18] A. G. Mal'shukov, V. V. Shlyapin, and K. A. Chao, Phys. Rev. B **66**, 081311(R) (2002).
[19] C. H. Chang, A. G. Mal'shukov, and K. A. Chao, cond-mat/0304508 (unpublished).
[20] D. Frustaglia, M. Hentschel, and K. Richter, Phys. Rev. Lett. **87**, 256602 (2001).
[21] M. Hentschel, H. Schomerus, D. Frustaglia, and K. Richter, Phys. Rev. B **69**, 155326 (2004).
[22] D. Frustaglia, M. Hentschel, and K. Richter, Phys. Rev. B **69**, 155327 (2004).
[23] A. Stern, Phys. Rev. Lett. **68**, 1022 (1992).
[24] A. G. Aronov and Y. B. Lyanda-Geller, Phys. Rev. Lett. **70**, 343 (1993).
[25] T.-Z. Qian and Z.-B. Su, Phys. Rev. Lett. **72**, 2311 (1994).
[26] D. Frustaglia and K. Richter, Found. Phys. **31**, 399 (2001).
[27] A. F. Morpurgo, J. P. Heida, T. M. Klapwijk, B. J. van Wees, and G. Borghs, Phys. Rev. Lett. **80**, 1050 (1998).
[28] J.-B. Yau, E. P. De Poortere, and M. Shayegan, Phys. Rev. Lett. **88**, 146801 (2002).
[29] We neglect the Dresselhaus spin-orbit coupling (Ref. 30) having in mind, e.g., InAs or InSb semiconductors where the Rashba interaction dominates (Ref. 31).
[30] G. Dresselhaus, Phys. Rev. **100**, 580 (1955).
[31] R. de Sousa and S. Das Sarma, Phys. Rev. B **68**, 155330 (2003).
[32] F. E. Meijer, A. F. Morpurgo, and T. M. Klapwijk, Phys. Rev. B **66**, 033107 (2002).
[33] T. Choi, S. Y. Cho, C.-M. Ryu, and C. K. Kim, Phys. Rev. B **56**, 4825 (1997).
[34] The correction (see Ref. 32) to the Hamiltonian used in earlier work consists in adding the last term in Eq. (2), which becomes negligible for large angular momentum ($\langle -i\partial/\partial\varphi + \phi/\phi_0 \rangle \gg 1$).
[35] See, e.g., that for large angular momentum the effective Rashba field $\mathbf{B}_R$ is determined by the second line of Eq. (2), corresponding to an effective radial field (i.e. (anti)parallel to $\hat{\mathbf{r}} = \cos\varphi\hat{x} + \sin\varphi\hat{y}$).
[36] For a review see, e.g., S. Datta, *Electronic Transport in Mesoscopic Systems* (Cambridge University Press, Cambridge, 1997).
[37] The Dirac notation refers only to the spin states. Here we assume that the particles escape from the ring after half a winding which holds true for strongly coupled leads. Below we will see that this actually provides a fairly good description of the conductance when comparing with complete 2D numerical quantum calculations. Moreover, our results agree with a related model for 1D rings based on a transfer matrix approach (including arbitrary winding numbers) which has been developed in parallel by B. Molnar, F. M. Peeters, and P. Vasilopoulos, Phys. Rev. B **69**, 155335 (2004).
[38] This makes sense since we see from Sec. II B that such pairs of spins are actually parallel.
[39] Y. Aharonov and A. Casher, Phys. Rev. Lett. **53**, 319 (1984).
[40] Note that the phase πQ_R is equivalent to the differential Rashba phase $\Delta\theta = \alpha_R(2m^*/\hbar^2)L$ acquired in a straight wire of length $L = \pi r_0$ (Refs. 5 and 41).
[41] F. Mireles and G. Kirczenow, Phys. Rev. B **64**, 024426 (2001).
[42] Y. Aharonov and J. Anandan, Phys. Rev. Lett. **58**, 1593 (1987).
[43] H. Mathur and A. D. Stone, Phys. Rev. Lett. **68**, 2964 (1992).
[44] This is based on the standard recursive method (Ref. 45) which uses a tight-binding model arising from the real-space discretization of the corresponding Schrödinger equation in a 2D geometry (Fig. 3). Here, the technique is generalized for including spin (Refs. 20, 22, and 46). This requires to replace the tight-binding on-site and hopping energies by 2×2 spin matrices and projecting the obtained Green function (matrix) onto transverse mode spinors (of incoming and outgoing states) in the leads for the calculation of the spin-dependent quantum transmission.
[45] See, e.g., D. K. Ferry and S. M. Goodnick, *Transport in Nanostructures* (Cambridge University Press, Cambridge, 1997).
[46] D. Frustaglia, Ph.D. thesis, TU Dresden, 2001.
[47] The number of incoming and outgoing open channels is kept constant within such energy window. Physically, the energy average can be associated either with an ensemble average on rings of slightly different size or, alternatively, with a finite temperature (sufficiently low for neglecting decoherence effects).
[48] Note that here the term *adiabatic* is used in a sense different from the one introduced previously in the context of adiabatic spin transport.
[49] The adiabatic switching of the Rashba coupling is introduced in order to avoid an abrupt transition between the region of interest subject to finite coupling (the ring) and the leads connected to reservoirs free of spin-orbit coupling. For a given energy, some differences can arise in the computed conductance when using or not the adiabatic switching in the case of strong Rashba coupling. However, no significant differences survive when performing an energy average in the way discribed above.
[50] D. Frustaglia and K. Richter (unpublished).
[51] Y. Meir, Y. Gefen, and O. Entin-Wohlman, Phys. Rev. Lett. **63**, 798 (1989).
[52] Y. Oreg and O. Entin-Wohlman, Phys. Rev. B **46**, 2393 (1992).
[53] Assuming (efficient) spin injection into semiconductors.
[54] Note the difference with respect to the Datta-Das proposal (Ref. 5), where incoming spin-polarized states point along the z or x axis to get spin oscillations.
[55] J. Schliemann, J. C. Egues, and D. Loss, Phys. Rev. Lett. **90**, 146801 (2003).